Some Aspects on the Zero-span Tensile Test

by R. Hägglund, P.A. Gradin and D. Tarakameh

ABSTRACT—In this paper, we present some analytical and numerical results concerning the zero-span testing method, frequently used for quality control of cellulose fiber for papermaking. Of particular interest is the relationship between an apparent modulus obtained from the zero-span testing method and the elastic properties of the fibers. The apparent elasticity modulus is estimated using two energy theorems in elasto-statics in which the role of span length is explored. Analytical results, derived under the assumption that slippage between specimen and clamps does not occur, clearly show that the apparent modulus strongly depends on the span length. This is verified by the numerical results obtained using the finite element method. In addition to the above analysis, the effect of slippage is investigated, also by utilizing the finite element method, and it is found that for a specific case, the contribution from slippage to the total displacement depends strongly on the length of the span. Tensile tests at nominal zero span were conducted in an effort to further validate the analysis with relevant experimental data and it was concluded that there is qualitative agreement between the experimental results and the result of the analysis.

KEY WORDS—Zero span, tensile test, fiber properties, friction

Introduction

It is generally agreed that both mechanical properties of the fibers and the strength of the fiber-to-fiber bonds govern the strength of paper materials. Consequently, it is desirable to be able to measure strength properties of cellulose fibers themselves in order to judge the quality of the raw material. However, single fiber testing is cumbersome and requires a large number of tests in order to reach statistical precision and is therefore not considered as being practical as a routine testing method. In recent years, interest has grown in the so-called zero-span (ZS) testing method for determining fiber strength. Hoffman Jacobsen introduced the concept of determining fiber strength from ZS measurements as early as 1925.[1] The idea was to obtain a measure of the fiber strength rather than the strength of the paper itself by conducting tensile tests of paper at a very short span length. This has been motivated by the assumption that the majority of fibers are clamped at both ends during loading. In the past 40 years, much work has been done in this field, by several investigators, mainly aiming to improve instrument design, develop measurement procedures and explain the fracture process.[2–7] In several publications it has been concluded that the method is likely a good indicator of fiber strength (e.g., Van Den Akker et al.[8] and Clark[9]).

Paper essentially consists of a stochastic network of discontinuous cellulose fibers and is usually manufactured by dewatering a cellulose fiber-suspension on a wire. The fibers have an inherent capability to form bonds between them without any additives. Since the fibers are much longer than the thickness of the paper sheet, the network is planar and almost two-dimensional. In machine-made papers, there are more fibers aligned in the machine direction than perpendicular to it. Consequently, at a macroscopic level, paper is often treated as being orthotropic, i.e., having different mechanical properties in three mutually perpendicular planes of symmetry.

A common tensile test of paper materials provides information on a series of mechanical properties. Standard tensile test methods are usually based on an ideal view of the physical problem. Namely, a slender specimen is subjected to an extension (usually at a constant extension rate) and the corresponding load is measured. The basic assumptions are that the loading is purely uni-axial and that the deformation takes place uniformly, both along the length of the specimen and throughout every cross-section. When both the elongation and the force are recorded, the stiffness, stress and strain at break can be determined. However, in the ZS test method, the span length is typically less than the thickness of the specimen.

Even without involving a theoretical treatment of the test method, it can be conjectured (according to the Saint Venant principle) that the stress state is non-uniform in the free span region.[10] Hence, evaluation techniques that are used for uni-axial testing are not generally applicable for evaluation of ZS test results. There is, however, an absence of work concerning the stress state developed in the thickness direction of the specimen during loading, a serious omission in view of its importance for the interpretation of the test results.

The aim of the present study is twofold. First, models which relate the apparent elastic modulus to the actual elastic modulus of the material and the span length are considered for a comparatively simple and well-defined case. Secondly, the influence of slippage between the specimen and the clamps is investigated. Additionally, an experimental investigation is carried out in order to verify the models.

Model

The present study addresses the mechanical response of a linear elastic paper during a tensile test with near zero span. It

R. Hägglund is a Research Leader at SCA Packaging Research, Box 716, S 851 21 Sundsvall, Sweden. P. A. Gradin (per.gradin@mh.se) is a Professor in Solid Mechanics and D. Tarakameh is a MSC Student, Mid Sweden University, S 851 70 Sundsvall, Sweden.

Original manuscript submitted: December 16, 2002.
Final manuscript received: March 12, 2004.
DOI: 10.1177/0014485104046085

might be argued that the assumptions on which the presented model is based are not at all realistic for a real situation. However, it is felt that if the ZS testing method can be shown to exhibit peculiarities in a well-defined situation, the introduction of large deformations, slippage, etc., is not likely to remove these peculiarities.

Problem Statement

A clamped specimen is studied. It is assumed that there is a small initial span between the two clamp-pairs, denoted s, in Fig. 1. In order to reduce the complexity of the model, it is assumed that the thickness of the specimen can be regarded as small compared to its width, so that a plane strain situation prevails. Thus, the stress and strain fields are dependent on x and y only, x being the coordinate in the loading direction and y oriented in the thickness direction of the specimen. Due to symmetry, only one quarter of the specimen (the upper-left quarter) is considered in the analysis and the origin of the coordinate system (x, y) is located in the lower-left corner of the reduced geometry. The dimension of the specimen is defined by the parameters s, L and t, i.e., span length, clamp length and half of the thickness of the specimen, respectively. All deformations are assumed to be small so that linear relations for equilibrium and kinematics are applicable.

For the part of the specimen compressed between the clamps, i.e., for $0 \leqslant x \leqslant L$, a two-dimensional orthotropic linear elastic constitutive relation is assumed, i.e.,

$$\sigma_x = C_{11}\varepsilon_x + C_{12}\varepsilon_y \tag{1a}$$

$$\sigma_y = C_{12}\varepsilon_x + C_{22}\varepsilon_y \tag{1b}$$

$$\tau_{xy} = C_{66}\gamma_{xy} \tag{1c}$$

where σ_x and σ_y are normal stresses in the x- and y-direction respectively and τ_{xy} is the shear stress in the xy-plane. ε_x and ε_y are normal strains in the x- and y-direction respectively and γ_{xy} is the shear strain in the xy-plane. C_{11}, C_{12}, C_{22} and C_{66} are elastic stiffness constants and can be related to engineering elastic constants, according to Appendix A1. Equations (1a)–(1c) can be expressed in the inverted form as

$$\varepsilon_x = S_{11}\sigma_x + S_{12}\sigma_y \tag{2a}$$

$$\varepsilon_y = S_{12}\sigma_x + S_{22}\sigma_y \tag{2b}$$

$$\gamma_{xy} = S_{66}\tau_{xy} \tag{2c}$$

where S_{11}, S_{12}, S_{22} and S_{66} are elastic flexibility constants. For the sake of simplicity, the material in the span region, i.e., for $L \leqslant x \leqslant L + s$, is assumed to obey a uni-axial constitutive relation according to

$$\sigma_x = E_s\varepsilon_x \tag{3}$$

where E_s is the effective modulus of elasticity in the loading direction in the free span domain. E_s can be related to the engineering elastic constants, as described in Appendix A1. The assumption of a region with uni-axial behavior is made since in some situations it is common to rewet the specimens prior to testing. Rewetting releases fiber-to-fiber bonds, which significantly reduces the coupling between in-plane and out-of-plane stresses in the material. With reference to Fig. 1, an apparent elastic modulus in the $x-$direction, E_{app}, can be defined as the ratio between the applied bulk stress σ_t and the mean strain ε_t, i.e.,

$$E_{app} = \sigma_t/\varepsilon_t \tag{4}$$

Upper Bound Solution for the Apparent Modulus

It is assumed that there is no slip between specimen and clamps during the process of loading. It is further assumed that the clamps can be regarded as rigid. If an admissible displacement field is used together with the theorem of minimum potential energy (cf. Fung[11]), an upper bound on the apparent modulus can be obtained. Using Fig. 1 for reference, the boundary conditions in this context are given by

$$u_y = 0 \quad \text{for} \quad 0 \leq x \leq L + s,\ y = 0 \tag{5a}$$

$$u_x = \varepsilon_t s, \quad \text{for} \quad x = L + s,\ 0 < y \leq t \tag{5b}$$

$$u_x = 0 \quad \text{for} \quad 0 \leq x \leq L,\ y = t \tag{5c}$$

In addition to the above conditions, u_y on the specimen/grip interface must not depend on x.

An admissible displacement field is continuous and satisfies boundary conditions on displacements. Again, with reference to Fig. 1, the following displacement field is assumed for the interval $0 \leqslant x \leqslant L$

$$u_x = f(x)(t^2 - y^2), \quad u_y = \varepsilon_{y0}y \tag{6}$$

where u_x and u_y are displacements in the x- and y-direction, respectively, and the function $f(x)$ and the constant ε_{y0} are to be determined. This is the displacement field with the simplest y dependence, satisfying the symmetry requirements. Since the main interest here is the apparent modulus, the clamping pressure σ_c can, due to assumed linearity, be put equal to zero. With the assumption of no slippage, this means that the faces of the paper specimen are assumed to be (adhesively say) bonded to the grips. By use of the compatibility relations, i.e.,

$$\varepsilon_x = \partial u_x/\partial x,\ \varepsilon_y = \partial u_y/\partial y,\ \gamma_{xy} = \partial u_x/\partial y + \partial u_y/\partial x \tag{7}$$

the following relationships are obtained for the strains:

$$\varepsilon_x = f'(x)(t^2 - y^2),\ \varepsilon_y = \varepsilon_{y0},\ \gamma_{xy} = -2yf(x). \tag{8}$$

A prime denotes differentiation with respect to x. The potential energy U for the model shown in Fig. 1 can now be expressed as

$$U = (1/2)\int_0^L\int_0^t (\sigma_x\varepsilon_x + \sigma_y\varepsilon_y + \tau_{xy}\gamma_{xy})\mathrm{d}x\mathrm{d}y + (sE_s/2)\int_0^t (\varepsilon_t - u_x(L, y)/s)^2\mathrm{d}y - \sigma_t\varepsilon_t ts. \tag{9}$$

The first integral expression on the right-hand side represents the elastic strain energy in the part of the specimen being in the clamp region and the second integral is the strain energy in the span region. The last term is the potential of the external

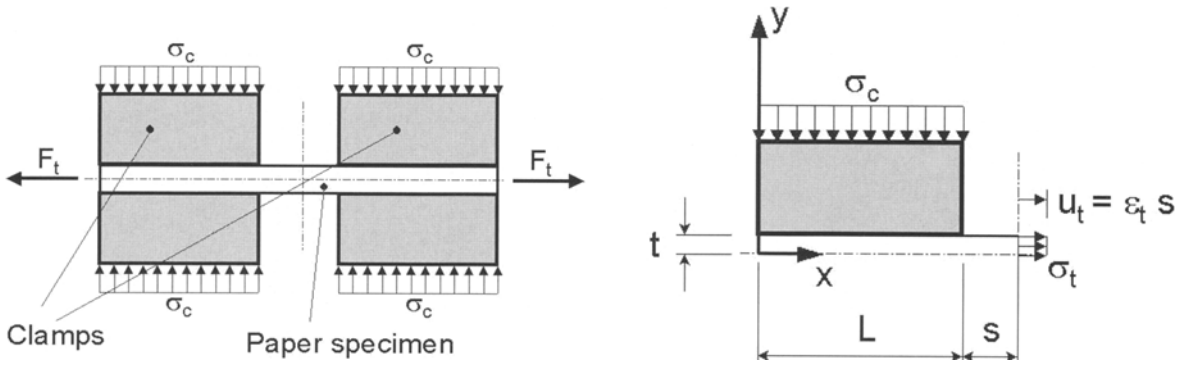

Fig. 1—Geometry of the testing device

loading. Note that, according to symmetry, the right paper specimen cross-section for the reduced geometry in Fig. 1 will remain plane. According to the theorem of minimum potential energy, the best displacement field is assumed to be one that makes U a minimum. A necessary condition for that is

$$\delta U = 0 \tag{10}$$

where δU is the first variation of U with respect to admissible variations $\delta f(x)$ and $\delta\varepsilon_{y0}$. Combining eqs (5a)–(5c), (8), (9) and (10) (for details concerning the variational procedure, see Berg and Gradin[15]) one will, after some lengthy algebra, arrive at a second-order differential equation with the solution

$$f(x) = A\cosh(\lambda x) + B\sinh(\lambda x) \tag{11}$$

where A and B are integration constants, λ is an eigenvalue (see Appendix A2) and cosh and sinh are the cosine and sine hyperbolic functions, respectively. Together with the solution for f, four natural boundary conditions result from the variational procedure. It can be shown (see Appendix A3) that the apparent modulus, E_{app}, will attain the value $E_s/6$ when s tends to zero. This value constitutes one upper bound for the apparent elastic modulus and, by including more unknown functions in the assumed displacement field (i.e., creating a more accurate displacement field), one can be certain that the apparent modulus at zero span will be less than $E_s/6$.

Lower Bound Solution for the Apparent Modulus

A lower bound on the apparent modulus can be obtained from the theorem of minimum complementary potential energy (cf. Fung[11]). Assume a stress field that satisfies the equilibrium equations and boundary conditions on stresses. The best stress field is assumed to be one that makes the complementary potential energy U_c a minimum. The equilibrium equations are:

$$\partial\sigma_x/\partial x + \partial\tau_{xy}/\partial y = 0 \tag{12a}$$

$$\partial\tau_{xy}/\partial x + \partial\sigma_y/\partial y = 0 \tag{12b}$$

It can be shown that the following stress field satisfies the equilibrium equations in $0 \leqslant x \leqslant L$

$$\sigma_x = g(x), \sigma_y = -g''(x)(t^2 - y^2)/2,$$
$$\tau_{xy} = -yg'(x) \tag{13a}$$

where $g(x)$ is an unknown function. In $L \leqslant x \leqslant L + s$, it is assumed that

$$\sigma_x = \sigma_t, \sigma_y = \tau_{xy} = 0. \tag{13b}$$

The following boundary conditions must be met:

$$\tau_{xy} = 0, \quad \text{for } 0 \leq x \leq L + s, y = 0 \tag{14a}$$

$$\sigma_x = \sigma_t, \tau_{xy} = 0, \quad \text{for } x = L, 0 \leq y \leq t \tag{14b}$$

$$\sigma_y = 0, \tau_{xy} = 0 \quad \text{for } L \leq x < L + s, y = t \tag{14c}$$

$$\sigma_y = 0, \quad \text{for } 0 \leq x \leq L, y = t \tag{14d}$$

$$\tau_{xy} = 0, \sigma_x = 0 \quad \text{for } x = 0, 0 < y \leq t. \tag{14e}$$

Note that the boundary condition on σ_y (which is identically satisfied) comes from the assumption of the clamping pressure σ_c being equal to zero. Equation (14b) comes from the assumption that σ_x is independent on y, so that the integral of σ_x through the thickness t will simply be $\sigma_x t$ which for equilibrium to prevail should equal $\sigma_t t$.

The complementary potential energy U_c is given by

$$U_c = (1/2)\int_0^L\int_0^t (\sigma_x\varepsilon_x + \sigma_y\varepsilon_y + \tau_{xy}\gamma_{xy})\mathrm{d}x\mathrm{d}y$$
$$+ (s/(2E_s))\int_0^t \sigma_x(L, y)^2\mathrm{d}y - \sigma_t\varepsilon_t ts. \tag{15}$$

By combining eqs (13) and (15) and by putting $\delta U_c = 0$ we have, after some lengthy algebra, a fourth-order differential equation with the solution

$$g(x) = A\cosh(\lambda_1 x) + B\sinh(\lambda_1 x) + C\cosh(\lambda_2 x)$$
$$+ D\sinh(\lambda_2 x) \tag{16}$$

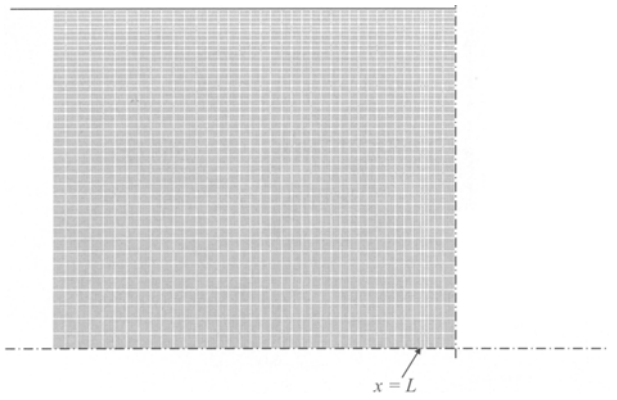

Fig. 2—Finite element mesh in the vicinity of the free span

where A, B, C and D are integration constants and λ_1 and λ_2 are eigenvalues (see Appendix A2). Combining the general solution (16) with the boundary conditions (14a)–(14e), a set of algebraic equations results, for the unknowns A, B, C, D and σ_t. Letting s approach zero, it can be shown that the apparent modulus, E_{app}, will tend to zero linearly with s so that for zero span a lower limit for the apparent modulus is zero.

Numerical Solution for the Apparent Modulus and Determination of Stress Profiles

The problem formulated in the sections "Problem Statement" and "Upper Bound Solution for the Apparent Modulus" is solved using the finite element analysis package ANSYS.[12] The purpose of the analysis is primarily to verify the accuracy of the upper and lower bound solutions, but also to study the stress gradients in the thickness direction. Additionally, a numerical solution conveniently enables evaluation of different material descriptions for the span region. For the sake of comparison, both a uni-axial constitutive relation, described by eq (3), and bi-axial, given by eqs (1a)–(1c), are used to describe the material response in the span region, i.e., for $L \leqslant x \leqslant L + s$. The first case is assumed to correspond to a situation when the fiber-to-fiber bonds are released in a wetting procedure prior to testing while the latter is believed to correspond to the response of a dry well-bonded paper specimen. The boundary conditions on displacements are given by eqs (5a)–(5c) and those on stresses are given in eqs (14a) and (14c)–(14e).

The model consists of 8200 quadrilateral plane-strain elements (PLANE42)[12] and the theory for small deformations is used. The PLANE42 element is defined by four nodes having two translational degrees of freedom each. The finite element mesh that is used is shown in Fig. 2.

Numerical Solution of a Model including "Slippage" Between Specimen and Clamps

It has been suggested[16] that the influence of slippage on the measured specimen elongation could be compensated for by performing a ZS test and an additional test at a significantly longer span, and subsequently using the displacement for the longer span to subtract the influence of slippage from the ZS data. Thus, it is tacitly assumed that the effect of slippage is independent of the span length. This assumption is addressed in this section. Another question of importance is how the stress gradient is affected by slippage. The boundary conditions (the boundary $0 < x < L$, $y = t$ is not included since it is a contact boundary) of the problem is given by

$$\tau_{xy} = 0, u_y = 0 \quad \text{for } 0 \leq x \leq L + s, y = 0 \tag{17a}$$

$$u_x = \varepsilon_t s, \tau_{xy} = 0 \text{ for } x = L + s, 0 \leq y \leq t \tag{17b}$$

$$\sigma_y = 0, \tau_{xy} = 0 \quad \text{for } L \leq x \leq L + s, y = t \tag{17c}$$

$$\tau_{xy} = 0, \sigma_x = 0 \quad \text{for } x = 0, 0 \leq y \leq t. \tag{17d}$$

In the region $0 \leq x \leq L$, $y = t$ the specimen is in contact with the clamp. It is again assumed that the clamps can be approximated as rigid bodies. The contact is taken into account in ANSYS by the Coulomb friction option,[12] i.e., the standard friction model with a constant coefficient of friction. In this model, the interaction between specimen and clamp is governed by a contact formulation (CONTA171 and TARGE169).[12] The material data, the finite element code, types of elements for describing the paper material, and the mesh used in this analysis are the same as for the "no-slippage" case. In addition to the quadrilateral elements, the model consists of 300 contact elements. The loading of the specimen consists of two steps. In the first step the clamping pressure is applied while the specimen outside the clamps is free to elongate. In the second step, the tensile load is applied while the clamping pressure is kept constant. A built-in iterative Newton–Raphson algorithm is used in the solution of governing incremental equilibrium equations.

Numerical Results

Some numerical examples are presented in this section. Material data, assumed to be realistic for a paper material, are listed in Table 1 and geometrical parameters are listed in Table 2. The analysis is carried out for a number of different span lengths, i.e., s is varied. Note that the parameters t and L are kept constant throughout the analysis.

For definition of E_x and E_y, etc., see Appendix 1.

TABLE 1—MATERIAL CONSTANTS

Material Constants	Values
E_x	5000 MPa
E_y	500 MPa
G_{xy}	91 MPa
ν_{xy}	0.5
ν_{xz}	0.25
ν_{yz}	0.5

TABLE 2—GEOMETRICAL CONSTANTS (WITH REFERENCE TO FIG. 1)

Geometrical Parameter	Values
L	2 (mm)
s	0.001–4 (mm)
t	0.042 (mm)

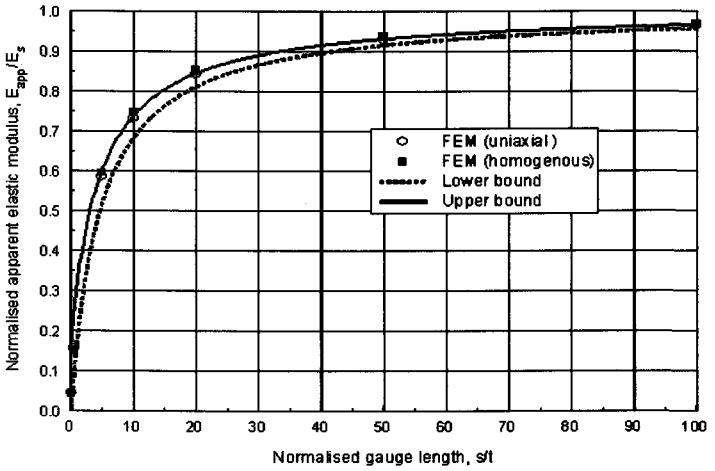

Fig. 3—Normalized apparent modulus versus normalized span length

Apparent Elastic Modulus

Figure 3 shows the normalized apparent E modulus as a function of the ratio between span and thickness. Both analytical and finite element results are given in the graph. Lower bound and upper bound denote the analytical lower and upper bound solutions of the apparent elastic modulus. FEM (uniaxial) refers to the case when the material in the span region is described by eq (3) and FEM (homogenous) the case when the span region is described by the same constitutive model as the clamp region, i.e., eq (1). The apparent modulus is here normalized with respect to E_s.

Stress Profiles in the Thickness Direction

Figure 4 shows the normalized stress profiles in the specimen at the cross-section $x = L$for three different span lengths. Normalized stress σ^* is here defined as

$$\sigma^* = \sigma_x(x = L, y)/\sigma_x(x = L, 0). \qquad (18)$$

This quantity indicates how many times larger the normal stress is in a point along the cross-section compared to the stress in the centre of the specimen. Hence, $\sigma^* = 1$ for all curves at $y = 0$. According to the graph, the stress field is very non-uniform and the stress gradient increases as the span decreases. In the point $y = t$, i.e., at the surface of the specimen, the normalized stress is 7.32, 48.3, and 112.0 for the s/t ratios 0.1, 5, and 50.

Effect of Slippage

Figure 5 shows, for three different values of the coefficient of friction μ and three different span lengths, the contribution from slippage to the total span elongation as a function of the applied tensile stress. The contribution from slippage is calculated from the difference in span elongation for the case when slippage is assumed and the case of no slippage, i.e., when an infinite coefficient of friction is assumed. An average clamping pressure of 40 MPa has been assumed in the calculations.

It can be observed that, at least for the cases presented, the contribution from slippage is not independent of the span length. For the shortest span length, slippage occurs already when the clamping pressure is applied. The fact that the distribution of the normal stress σ_x over the cross section $x = L$ is very non-uniform when there is no slippage between the specimen and the clamp has been shown. However, Fig. 6 shows that, even though there is a tendency for the stress-profile to become relatively flatter when the load is increased, the stress is still far from being uniform when slippage is included in the model.

Experimental Details

Experiments were conducted in an effort to gain additional insight into how the span length affects the load–deformation response of a paper material tested at nominal zero span.

Test Method and Specimen Preparation

Tensile tests were performed using a type of clamp specially designed for tensile testing at extremely short span length. The design of the clamps is similar to the design described by Clark[9] (see Appendix A4). The difference is mainly that the clamp pressure is accomplished by a hydraulic piston instead of spring loaded clamp screws. The clamps were mounted in a MTS Universal Testing Machine. Prior to applying clamp pressure, the clamps were brought together creating a nominal zero span. During testing, the specimen was loaded at a constant crosshead speed of 1 mm min^{-1} and both displacement and load were monitored and recorded. The load was measured by the load cell and elongation by the moving crosshead. In order to obtain optimal accuracy, the compliance of the load frame and clamping arrangement was taken into account in the evaluation of the elongation of the specimen. The tests were conducted on a commercial copy paper, having grammage, i.e., surface weight, of 85 g m^{-2} and made of a chemical pulp. The thickness of the sheet was 105 μm. Standard methods from the Scandinavian Pulp,

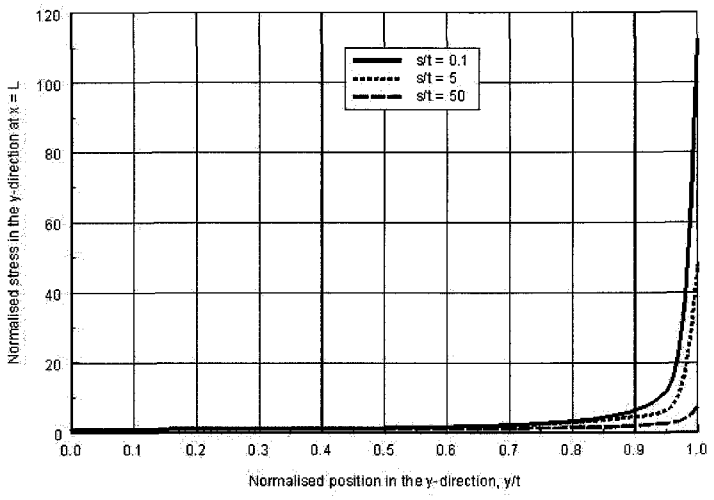

Fig. 4—Normalized normal stress profiles at x = L for s/t = 0.1, 5, and 50

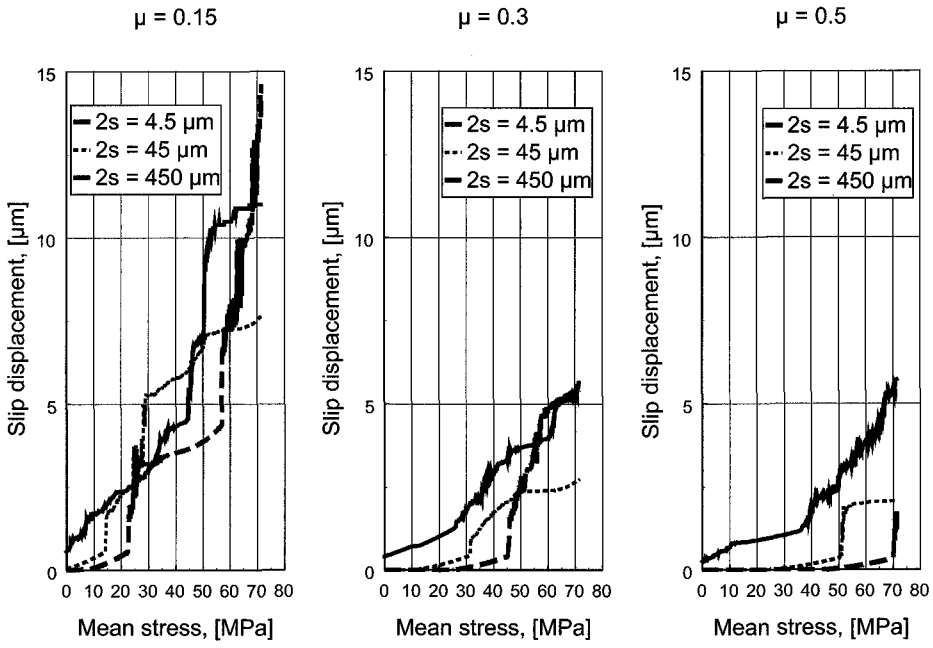

Fig. 5—Contribution from slippage to the span elongation

Paper and Board Testing Committee (SCAN) were used to test the structural properties. The standards used are SCAN-P7:96 for thickness, and SCAN-P6:75 for basis weight.

The material was tested in the cross-direction, i.e., perpendicular to the manufacturing direction.

In order to study the effect of varying the thickness of the specimen, tests were carried out where multi-ply specimens were used, i.e., where each specimen consisted of one or several layers of paper stacked on top of each other, see Fig. 7. The number of layers was varied. One, two, three, four, five, and ten layers were tested. The climate used was 23°C and 50% RH and is in accordance with SCAN-P2:75 1975.[13] The specimens were conditioned for at least 48 h in this climate prior to testing and the clamping pressure was estimated to be 40 MPa. Now, since the layers are not glued together there is a possibility for relative movement between the layers, which will give a situation different from what one will have if a homogeneous paper sample is considered. However, from the finite element method results in Fig. 3 it can be seen that at least the apparent modulus is almost the same for the

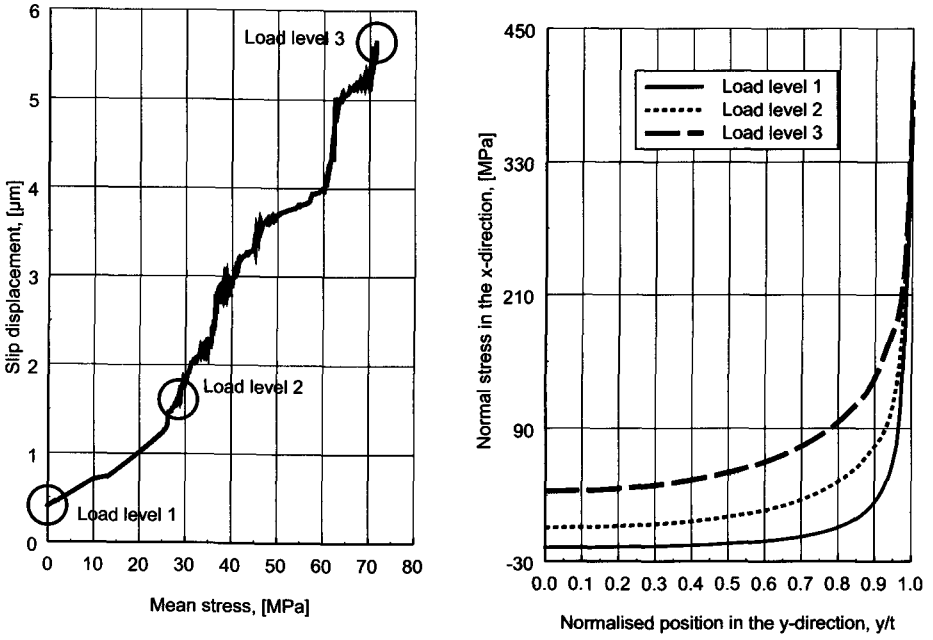

Fig. 6—Longitudinal stress over the cross-section $x = L$, $\mu = 0.3$ and $2s = 4.5$ μm

uni-axial (completely independent layers) and the homogeneous case, which might support the fact that the numerical and experimental results can be compared.

Experimental Results

Figure 8 shows the load–deformation curve for the case when several stacked paper sheets are tested at an extremely short span length. Here, the average force on each paper layer is plotted against the deformation. This average force may be interpreted as average stress acting in the loading direction of the specimen. The results show that peak load decreases as the number of layers increases. Further, the displacement at peak load increases as the number of layers is increased. The experimental results reported are limited to CD. However, similar "overall" load–displacement response has been observed for tests in MD for the same paper material, and also for handmade isotropic sheets.

In Fig. 9, the initial part of the load–deformation curve has been magnified and a straight line has been fitted to experimental data. Note that the slope of the line decreases for an increasing number of layers. Hence, assuming that the very small initial span is independent of the thickness of the specimen, i.e., number of layers, the apparent modulus strongly depends on the thickness of the specimen.

Discussion and Conclusions

It has been shown analytically (and confirmed using finite element analyses) that, in one particular situation, i.e., when there is no slippage and when linear elastic material behavior can be assumed, the ZS testing method has some inherent problems in that the apparent modulus of elasticity depends strongly on the span length and that the stress field in the specimen is far from uniform, for near ZS lengths. It has been shown that E_{app} will be in the interval $[E_s/6, 0]$ for a span length equal to zero.

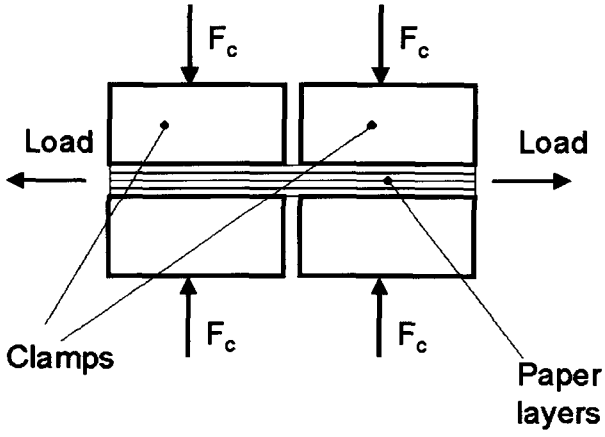

Fig. 7—Schematic diagram of the specimen configuration

If it is accepted that the apparent modulus and the measured fracture strain are dependent not only on the true material properties but also on the geometry, this complicates the evaluation of the material properties. For instance, two paper specimens having identical properties but with different thickness will show different apparent modulus at a given span length. This effect was observed in the experimental part of this study. Further, if the two specimen types are loaded until failure the thinner specimen will most likely exhibit a relatively high breaking stress because of a flatter stress profile. The latter is to some extent supported by the experimen-

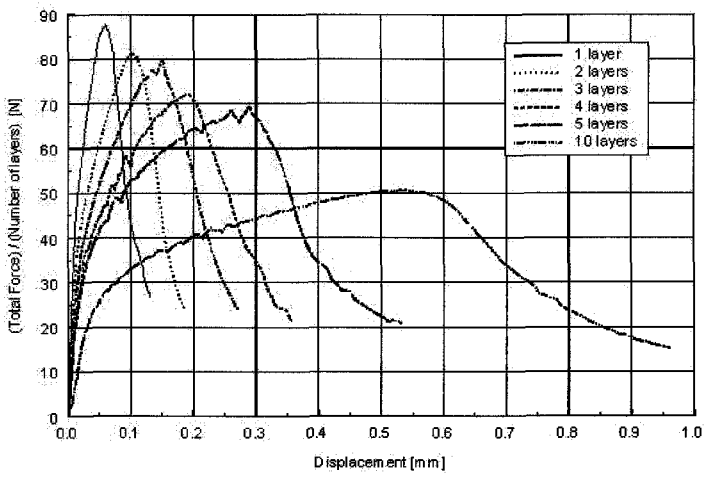

Fig. 8—Stress–displacement curve (load on the crosshead divided by the number of layers)

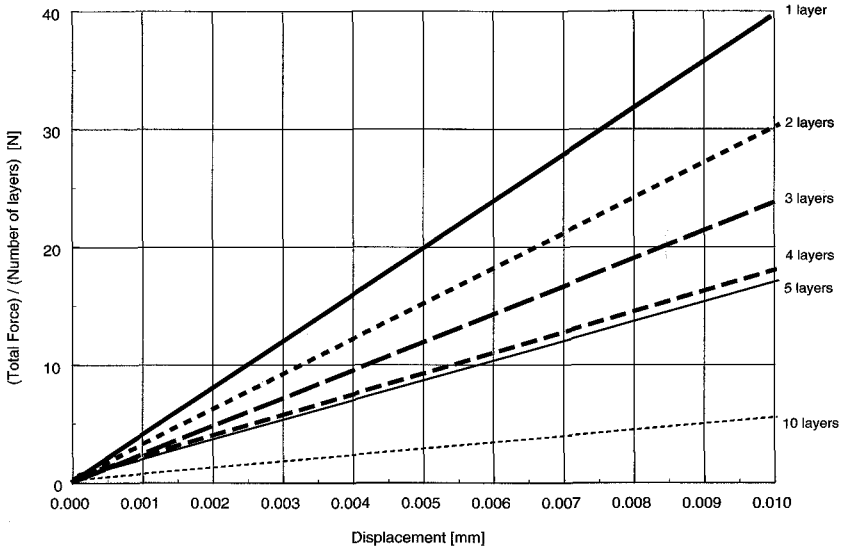

Fig. 9—Initial slope of the stress–displacement curve

tal results presented in this paper and also in an earlier work by Wink et al.,[14] where it was found that the ZS strength decreases for increasing surface weight at surface weights above 60 g m^{-2}.

It can be argued that these conclusions are based on a model which is not adequate for a real situation. However, it is unlikely that the introduction of large deformations, nonlinear material behavior, etc., would remove all problems discussed above.

Furthermore, since slippage is likely to occur at some stage of loading, a finite element analysis with slippage included was carried out. It was found from this analysis that the contribution from slippage to the total span elongation depended strongly on the span length, thus making uncertain any evaluation scheme assuming the opposite. For the non-slippage model, it has been assumed that that the material in the span region can be regarded as a number of independent layers. This was done in order to obtain analytical models amenable to relatively simple calculations. It was shown through a finite element analysis of a specific case that the conclusions based on this assumption will probably hold also for the case when the material in the span region is homogeneous, i.e., when the fibers are perfectly bonded. To conclude, the remedy for most of the objections raised in this paper would be to use a very large s/t ratio, i.e., for a given span length to use as thin a paper specimen as possible.

Appendix A1

With reference to Fig. 1, E_x and E_y are the elasticity modules in the x- and y-direction, respectively, and G_{xy} is the shear modulus in the x–y plane. ν_{xy}, ν_{xz} and ν_{yz} are the Poisson ratios. In particular, ν_{xy} is defined as minus the ratio between the strain in the y-direction and the strain in the x-direction, when the paper material is loaded in the x-direction only. The z-direction is orthogonal to the x- and y-directions.

Stiffness and Flexibility Constants in Terms of Engineering Constants

By putting the strain in the z–direction, ε_z, equal to zero in the general orthotropic constitutive relation, it is straightforward to derive the plane strain relations.

Stiffness constants:

$$C_{11} = 1/(E'_y(1/(E'_x E'_y - \nu'^2_{xy}/E^2_x)$$

$$C_{22} = 1/(E'_x(1/(E'_x E'_y - \nu'^2_{xy}/E^2_x)$$

$$C_{12} = C_{21} = \nu'_{xy}/(E_x(1/(E'_x E'_y - \nu'^2_{xy}/E^2_x)$$

$$C_{66} = G_{xy}$$

and flexibility constants:

$$S_{11} = 1/E'_x$$

$$S_{22} = 1/E'_y$$

$$S_{12} = S_{21} = -\nu_{xy}/E'_x$$

$$S_{66} = 1/G_{xy}$$

where

$$E'_x = E_x/(1 - \nu_{zx}\nu_{xz})$$

$$E'_y = E_y/(1 - \nu_{zy}\nu_{yz})$$

$$\nu'_{xy} = \nu_{xy} + \nu_{zy}\nu_{xz}.$$

Relation Between "Effective" Modulus E and Engineering Constants

Assuming that the strain in the z-direction and the stress in the y-direction are zero, we obtain

$$E_s = E_x/(1 - \nu_{zx}\nu_{xz}).$$

Appendix A2

Determination of the Eigenvalues

Upper bound

The eigenvalue, λ for the upper bound problem is defined by the following relation

$$\lambda = \sqrt{4C_{66}I_3/(C_{11}I_1)}$$

where

$$I_1 = \int_0^t (t^2 - y^2)^2 dy = 8t^2/15$$

$$I_3 = \int_0^t y^2 dy = t^3/3.$$

Lower bound

The eigenvalues, λ_1 and λ_2, for the lower bound problem are defined by the following relation

$$\lambda_{1,2} = \sqrt{\alpha \pm \sqrt{\alpha^2 + \beta^2}}$$

where

$$\alpha = 2(S_{12}I_2 + S_{66}I_3)/(S_{22}I_1)$$

$$\beta = 4S_{11}t/(S_{22}I_1)$$

and

$$I_1 = \int_0^t (t^2 - y^2)^2 dy = 8t^2/15$$

$$I_2 = \int_0^t (t^2 - y^2) dy = 2t^3/3$$

$$I_3 = \int_0^t y^2 dy = t^3/3.$$

Appendix A3

The four natural boundary conditions obtained through the variational procedure are

$$C_{12}I_2(f(L) - f(0)) + C_{22}tL\varepsilon_{y0} = 0$$

$$C_{12}I_2\varepsilon_{y0} + C_{11}I_1 f'(0) = 0$$

$$C_{12}I_2\varepsilon_{y0} + C_{11}I_1 f'(L)E_s I_2\varepsilon_t + E_s I_1 f(L)/s = 0$$

$$E_s st\varepsilon_t - E_s I_2 f(L) = \sigma_t st.$$

I_1 and I_2 are defined in Appendix 2. With the solution for f, i.e., eq (11), the natural boundary conditions will become

$$A(\cosh(\lambda L) - 1) + B\sinh(\lambda L) + C_{22}tL\varepsilon_{y0}/(C_{12}I_2) = 0$$

$$C_{12}I_2\varepsilon_{y0} + C_{11}I_1\lambda B = 0$$

$$A(C_{11}\lambda\sinh(\lambda L) + E_s\cosh(\lambda L)/s) + B(C_{11}\lambda\cosh(\lambda L) + E_s\sinh(\lambda L)/s) + C_{12}I_2\varepsilon_{y0}/I_1 - E_s I_2\varepsilon_t/I_1 = 0$$

$$A\cosh(\lambda L) + B\sinh(\lambda L) - st\varepsilon_t/I_2 = -\sigma_t st/(E_s I_2).$$

If it is assumed that A, B and ε_{y0} depend linearly on s and that ε_t is independent of s, this would be consistent with the first,

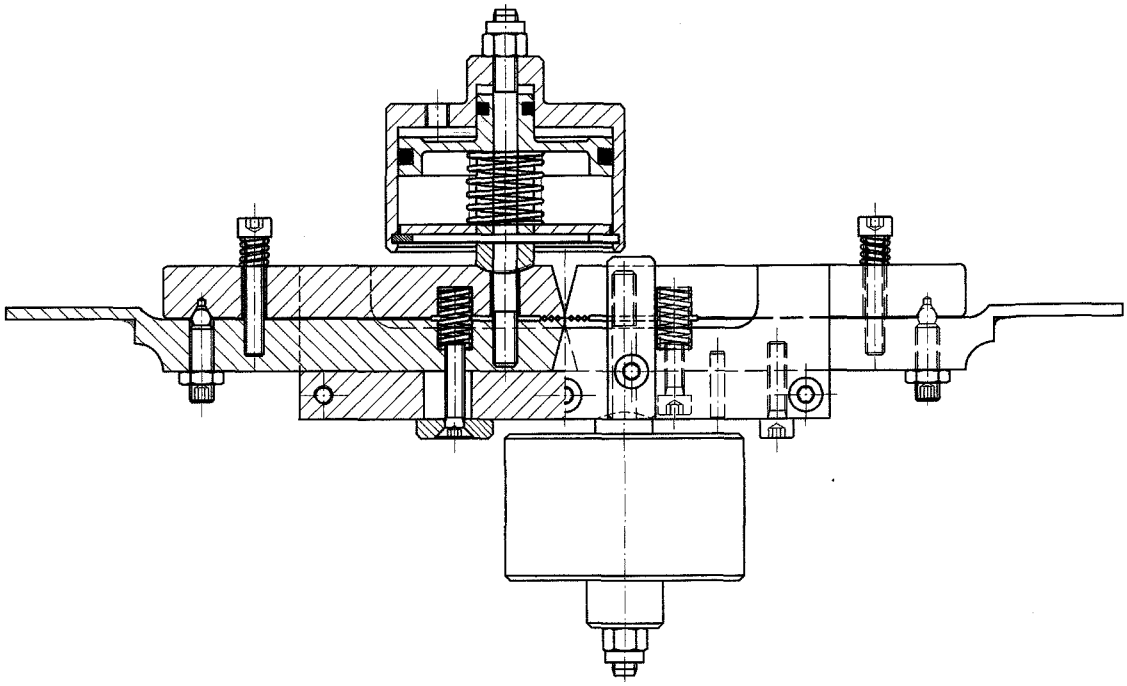

Fig. A1—Drawing of the clamps

second and fourth equations but not, in general, with the third equation. However, when s approaches zero, the assumption will be consistent with the third equation also. Utilizing the above assumption and by letting s approach zero, the third and fourth equations will give

$$\left(\frac{I_2}{I_1} - \frac{t}{I_2}\right)\varepsilon_t = -\sigma_t t/(E_s I_2)$$

and by the definitions of I_1 and I_2 we will obtain

$$\sigma_t/\varepsilon_t = E_s/6.$$

Appendix A4

Figure A1 shows the design of the clamps used in the experiments. A side view of the clamping arrangement is shown. The design of the clamps is essentially the same as was described by Clark.[9] The main improvement is that the clamp pressure is applied by two pneumatic cylinders, instead of spring loaded clamping screws.

Acknowledgment

Professor Myat Htun is acknowledged for valuable discussions regarding the ZS testing method.

References

1. *Hoffmann Jacobsen, P.M., Paper Trade Journal,* **81** *(22), 52 (1925).*

2. *Boucai, E., "Zero-Span Tensile Test and Fiber Strength," Pulp and Paper Magazine Canada,* **72** *(10), 73–76 (1971).*

3. *Cowan, W.F. and Cowdrey, E.J., "Evaluation of Paper Strength Components by Short-Span Tensile Analysis," Tappi Journal,* **57** *(2), 90–93 (1974).*

4. *El-Hosseiny, F. and Bennet, K., "Analysis of the Zero-Span Tensile Strength of Paper," Journal of Pulp Paper Science,* **11** *(4), J121–J127 (1985).*

5. *Gurnagul, N. and Page, D.H., "The Difference Between Dry and Rewetted Zero-Span Tensile Strength of Paper," Tappi Journal,* **72** *(12), 164–167 (1989).*

6. *Cowan, W., "Rapid Testing of Fiber Quality in Machine-Made Paper," Pulp and Paper Canada, 91 (2), T57–T60 (1990).*

7. *Cowan, W.F., "Testing Pulp Quality—An Alternative to Conventional Laboratory Evaluation," Tappi Journal, 77 (10), 77–81 (1994).*

8. *Van Den Akker, J.A., Lathrop, A.L., Voelker, M.H., and Dearth, L.R., "Importance of Fiber Strength to Sheet Strength," Tappi Journal,* **41** *(8), 416–425 (1958)*

9. *Clark, J. d'A., "The Ultimate Strength of Pulp Fibers and Zero-Span Tensile Test," Paper Trade Journal,* **118** *(1), 29 (1944).*

10. *Cook, R.D. and Young, W.C., Advanced Mechanics of Materials, Macmillan, New York (1985).*

11. *Fung, Y.C, Foundations of Solid Mechanics, Prentice-Hall, Englewood Cliffs, NJ (1965).*

12. *Ansys User's Manual, Swanson Analysis System Inc., Houston, PA (1997).*

13. *SCAN-P2:75, Paper and Board-Conditioning of Test Specimens (1975).*

14. *Wink, W.A. and Esperen, R.H.V., "The Development of an Improved Zero-Span Tensile Test," Tappi Journal,* **45** *(1), 10 (1962).*

15. *Berg, J.E. and Gradin, P.A., "A Micromechanical Model of the Deterioration of a Wood Fiber," Journal of Pulp and Paper Science,* **25** *(2), 66–71 (1999).*

16. *Batchelor, W.J. and Westerlind, B.S., "Measurement of Short Span Stress–Strain curves of Paper," Nordic Pulp Paper Research Journal,* **18** *(1), 44–50 (2003).*